Journal of Statistical Physics, Vol. 113, Nos. 5/6, December 2003 (© 2003)

Boundary Effects on Exact Solutions of the Lagrangian-Averaged Navier–Stokes-α Equations

Darryl D. Holm,[1] Vakhtang Putkaradze,[2] Patrick D. Weidman,[3] and Beth A. Wingate[4]

Received September 12, 2002; accepted May 16, 2003

In order to clarify the behavior of solutions of the Lagrangian-averaged Navier–Stokes-α (LANS-α) equations in the presence of solid walls, we identify a variety of exact solutions of the full equations and their boundary layer approximations. The solutions demonstrate that boundary conditions suggested for the LANS-α equations in the literature[(1)] for a bounded domain do not apply in a semi-infinite domain. The convergence to solutions of the Navier–Stokes equations as $\alpha \to 0$ is elucidated for *infinite-energy solutions* in a semi-infinite domain, and non-uniqueness of these solutions is discussed. We also study the boundary layer approximation of LANS-α equations, denoted the Prandtl-α equations, and report solutions for turbulent jets and wakes. Our version of the Prandtl-α equations includes an extra term necessary to conserve linear momentum and corrects an earlier result of Cheskidov.[(2)]

KEY WORDS: Fluid dynamics; exact solutions; boundary layers; turbulence; jets; wakes; stagnation.

1. INTRODUCTION

A set of candidate closure equations for the theory of turbulence in several classical flows are examined in this study. These are the LANS-α equations

[1] Theoretical Division and Center for Nonlinear Studies, Los Alamos National Laboratory, Los Alamos, New Mexico 87545 and Mathematics Department, Imperial College of Science, Technology and Medicine, London SW7 2AZ, United Kingdom; e-mail: dholm@lanl.gov

[2] Department of Mathematics and Statistics, University of New Mexico, Albuquerque, New Mexico 87131-1141; e-mail: putkarad@math.unm.edu

[3] Department of Mechanical Engineering, University of Colorado at Boulder, Boulder, Colorado 80309-0427; e-mail: Patrick.Weidman@colorado.edu

[4] Computer and Computational Sciences Division, Los Alamos National Laboratory, Los Alamos, New Mexico 87545; e-mail: wingate@lanl.gov

0022-4715/03/1200-0841/0 © 2003 Plenum Publishing Corporation

for the Lagrangian-averaged turbulent flow velocity $\mathbf{u}(\mathbf{x}, t)$ reported in ref. 3, *viz.*

$$\frac{\partial \mathbf{v}}{\partial t} + (\mathbf{u} \cdot \nabla)\, \mathbf{v} + \beta\, \nabla \mathbf{u}^T \cdot \mathbf{v} = -\frac{1}{\rho_0} \nabla p + \Lambda\, \Delta \mathbf{v}, \qquad \mathbf{v} = (1 - \alpha^2 \Delta)\, \mathbf{u}, \qquad \nabla \cdot \mathbf{u} = 0. \tag{1}$$

The parameter α (assumed constant for now) is the filtering length scale. In those original papers the dissipation coefficient Λ was assumed equal to the fluid kinematic viscosity ν. In ref. 3, the steady solutions of (1) were computed for flows in pipes and channels. These solutions were in excellent agreement with the experiments of Wei and Willmarth[4] (channel flows) and Zaragola[5] (pipe flows) over the entire available range of Reynolds numbers. However, a recent study[6] showed that, in general, $\Lambda > \nu$ may be determined from experimental data; we note that introduction of the dissipation coefficient Λ does not change the results of ref. 3.

Nondimensionalizing the LANS-α equations using length scale L_* and velocity scale U_* shows that the coefficient multiplying the dissipation term becomes Re^{-1}, where $\mathrm{Re} = U_* L_* / \Lambda$ is the Reynolds number based on Λ. Setting $(\alpha, \beta) = (0, 0)$ reduces (1) to the Navier–Stokes equations. Setting $(\alpha, \beta) = (\mathrm{const}, 0)$ gives a variant of Leray's regularization of the Navier–Stokes equations.[7] We note that the results of ref. 3 for the comparisons with turbulence in channels and pipes apply equally to both $\beta = 1$ and $\beta = 0$. Because of its origins in refs. 8 and 9, without viscosity, the LANS-α model (1) is also known as the viscous Camassa–Holm equations (VCHE).[1, 3, 10] In what follows, we shall always assume $\beta = 1$.

The goal of our study is to analyze the effect of solid boundaries on solutions of the LANS-α equations. At solid boundaries, Dirichlet (no-slip) boundary conditions on the velocity are imposed. However, application of $\mathbf{u} = 0$ at a boundary is not sufficient for the problem to be well-posed. This may be illustrated by the simple example of planar Poiseuille flow along the streamwise direction x in a channel $-L \leqslant y \leqslant L$. Upon assuming a fully developed flow $\mathbf{u} = [U(y), 0]$, Eq. (1) simplifies to

$$U'' - \alpha^2 U'''' = A \tag{2}$$

with boundary conditions $U(-L) = U(L) = 0$. Clearly, $U(y)$ cannot be determined from the no-slip boundary conditions alone, since (2) is of fourth order. In ref. 3, this problem was closed by requiring the solution $U(y)$ to be symmetric: $U(y) = U(-y)$. While this is in agreement with experimental data for the straight channel, this symmetry requirement is not applicable for more general flows. For instance, flow through an

expanding channel exhibits symmetry-breaking.[11] Thus, it is of interest to find other boundary conditions to be imposed at solid boundaries. This was initiated by Marsden and Shkoller[1] but, as we show below using explicit examples, the boundary conditions suggested in ref. 1 for *finite-energy* solutions in bounded domains need to be modified for *infinite-energy* solutions in unbounded domains.

In the current investigation, we consider semi-infinite fluid domains and require physically relevant behavior of solutions far from the wall. This furnishes some well-posed problems which we are able to solve in closed form. For the full LANS-α equations, solutions of two stagnation-point flows and the flow generated by a rotating disk are determined, while for their boundary layer variant, solutions for planar jets and wakes are found. In the case of the stagnation-point flows for LANS-α, we discover that the stationary solutions are not unique. This has some interesting implications for the behavior of solutions of the full LANS-α as $\alpha \to 0$. For example, the non-uniqueness caused by the presence of the walls might not be unphysical, since the Navier–Stokes equations also exhibit non-uniqueness of stationary solutions in many geometries involving solid walls.

The paper is organized as follows. Exact solutions describing stagnation-point flows are given in Section 2. Explicit solutions for planar and axisymmetric stagnation-point flows are derived, and a discussion of oblique planar stagnation-point flow is given. Section 3 deals with the swirling flow generated by a rotating disk. To make further progress in the analysis of the wall effects, Section 4 is devoted to the derivation of the boundary layer approximation to the LANS-α equations. In briefly outlining the derivation, we correct the equations of Cheskidov[2] to restore conservation of linear momentum. The corrected Prandtl-α equations are then used to describe planar turbulent wakes and jets, and reasonable corroborations of solutions with experiments are observed.

2. STAGNATION-POINT FLOWS

2.1. Stagnation Point Flows: Normal Incidence

Consider a two-dimensional stagnation-point flow impinging normally to a flat wall placed at $y = 0$. In terms of the streamfunction $\Psi(x, y)$ for which the velocity components (u_x, u_y) are given by $(\partial\Psi/\partial y, -\partial\Psi/\partial x)$, the outer potential flow $\Psi_0 = axy$ is characterized by the strain rate a from which the characteristic length $L = \sqrt{\Lambda/a}$ can be formed. Re-scaling the spatial coordinates with this length, $(x, y) = \sqrt{\Lambda/a}\,(X, Y)$, yields for the outer potential flow $\Psi_0 = \Lambda XY$.

Since this streamfunction does not satisfy the no-slip boundary condition $u_x = 0$ at $y = 0$, we follow Heimenz[12] and seek a solution of the LANS-α equations in the form $\Psi = \Lambda X f(Y)$ that matches the outer potential flow as $Y \to \infty$. Equations (1) yield the fifth-order ODE for $f(Y)$ with $F = f - \tilde{\alpha}^2 f''$

$$F''' + fF'' - (1+\beta)\, f'F' + \beta(f'^2 - \tilde{\alpha}^2 f''^2) + 1 = 0 \tag{3}$$

where $\tilde{\alpha} = \alpha\sqrt{a/\Lambda}$ and the prime denotes differentiation with respect to Y. Imposing the no-slip boundary condition at the impermeable wall and matching in the far field require

$$f(0) = 0, \qquad f'(0) = 0, \qquad \lim_{Y\to\infty} f'(Y) = 1. \tag{4}$$

The Heimenz equation for stagnation-point NS flow is obtained by setting $\tilde{\alpha} = \beta = 0$ in (3). In this case, $F = f$ and the order of the equation is reduced by two.

The three boundary conditions (4) are sufficient to find the solution to the original *third* order Heimenz equation. On first sight, it appears there are an insufficient number of conditions to solve the *fifth* order Heimenz-α equation (3). However, the boundary condition of asymptotic matching $f'(\infty) = 1$ admits the additional boundary conditions

$$\lim_{Y\to\infty} f''(Y) = 0, \qquad \lim_{Y\to\infty} f'''(Y) = 0. \tag{5}$$

We choose these in particular because the Heimenz solution for laminar flow approaches the asymptote monotonically, and we expect similar behavior from the Lagrangian-averaged turbulent flow solutions.

The system (3)–(5) has the single dimensionless parameter $\tilde{\alpha}$ taken here as a constant. A theorem[1, 10] states that when $\alpha \to 0$, the solution of the LANS-α equations converges to a solution of the Navier–Stokes equations. This theorem, however, was derived for flows in either periodic, or bounded domains, and may be violated in semi-infinite domains where solid walls are present and the solution has infinite energy. In particular, an analytical solution to the Heimenz-α flow is

$$f(Y) = Y + \tilde{\alpha}(e^{-Y/\tilde{\alpha}} - 1), \tag{6}$$

$$u_x = X(1 - e^{-Y/\tilde{\alpha}}), \qquad u_y = Y + \tilde{\alpha}(e^{-Y/\tilde{\alpha}} - 1). \tag{7}$$

It is clear that, in the limit of $\tilde{\alpha} \to 0$, solution (7) does not converge to the standard Heimenz solution. In fact, it does not have a well-defined regular

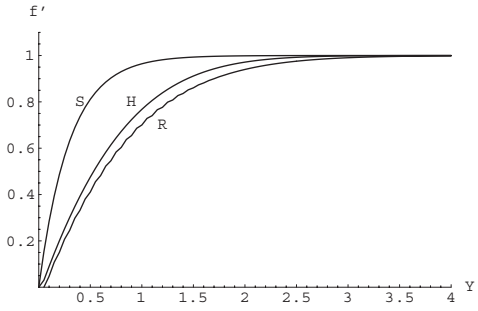

Fig. 1. Velocity function $f'(Y)$ for Heimenz-α flow computed for $\tilde{\alpha} = 0.3$. H: Heimenz solution, R: regular solution, S: singular solution (6).

limit as $\tilde{\alpha} \to 0$. We therefore call this solution *singular* and denote it with the letter S in Fig. 1. It is also clear that for the solution (7), the action of the Stokes operator (Stokesian) on the velocity at the wall is not zero, but is equal to $(X/\tilde{\alpha}^2, 1/\tilde{\alpha}^2)$. This is in contradiction with the result of Marsden and Shkoller[1] for bounded domains, stating that the Stokesian of the velocity at a solid wall must be equal to zero.

It is interesting to note that another solution of (3)–(5) exists which does converge to the Heimenz solution. This velocity function $f(Y)$ can be found numerically by continuation in α from the Heimenz solution ($\alpha = 0$). We call this solution *regular* and denote it with the letter R in Fig. 1. Finally, the Heimenz solution ($\alpha = 0$), denoted by the letter H, is included in this figure for comparison.

We conjecture that only the regular solution should be considered the physically correct solution. Thus, if a theorem about the existence of stationary solutions and convergence as $\alpha \to 0$ were possible to prove in the presence of walls, it should state that there is at least one solution of the LANS-α equations that converges to the solution of the Navier–Stokes equations as $\alpha \to 0$. Our explicit examples show that proof of a more general result, that *all* solutions of the LANS-α equations converge to the corresponding solution of the Navier–Stokes equations, will not be possible in general. The lack of convergence as $\alpha \to 0$ is not because the domain is unbounded. One may prove, for example, that the solutions of the LANS-α models converge to solutions of the Navier–Stokes in $\mathbb{R}^n$, provided these solutions have *finite* "*energy*" (that is, finite H^1 and L^2 norms). The solutions discussed here do not converge to those of the Navier–Stokes equations because these solutions have infinite energy (H^1 and L^2 norms). The convergence theorem proved in [10, 1] states that convergence takes place in a norm or weak topology, which involves the L^2 norms of the solutions.

However, the solutions to the alpha models presented here are *not* in L^2. Consequently, defining their convergence in the sense of extracting a bounded subsequence in the L^2 norm, etc., is not possible. In fact, the solutions established here were not envisioned in the original derivation of the alpha models. The alpha models were derived using Hamilton's variational principle, in which the kinetic energy is the square of the H^1 Sobolev norm. In that derivation, the solutions were expected to belong to H^1 and hence to L^2. However, the solutions presented here do not fulfill this expectation. Instead, the solutions established here transcend the class that was originally expected in the derivation of the alpha models. Additional investigations will be pursued elsewhere for this new class of solutions, which satisfy the alpha model equation, but not the variational principle used in its derivation.

2.2. Stagnation Point Flows: Oblique Incidence

The Heimenz-α equation may be generalized to an oblique stagnation-point flow. This generalization was first discovered by Stuart[13] and then rediscovered independently by Tamada[14] and Dorrepaal.[15] The main idea is to notice that a family of stream-functions of the form $\Psi_0 = \Lambda(XY + kY^2/2)$ describes a potential stagnation-point flow with slanted streamlines. The slope of streamlines at infinity is proportional to the dimensionless parameter k. Again, this flow does not satisfy the boundary conditions at the wall, so a modified streamfunction of the form

$$\Psi = \Lambda[Xf(Y) + kg(Y)] \tag{8}$$

is posited. Substituting expression (8) into the LANS-α equations shows that the function $f(Y)$ satisfies Heimenz-α equation (3) while the function $g(Y)$ satisfies the following linear sixth-order ODE, where as before $F = f - \tilde{\alpha}^2 f''$, and now $G = g - \tilde{\alpha}^2 g''$,

$$(G''' + fG'' - (1+\beta)\, f'G')' = -\beta(F'g'' + f''G'). \tag{9}$$

Boundary conditions for $g(Y)$ are the no-slip conditions at the wall and the far field asymptotic matching conditions, namely

$$g(0) = 0, \qquad g'(0) = 0, \qquad \lim_{Y\to\infty} g''(Y) = 1. \tag{10}$$

The modified streamfunction Ψ describes a stagnation-point flow with streamlines inclined at angle arc $\tan(1/k)$ relative to the wall. Again, the

asymptotic matching condition at $Y = \infty$ admits additional boundary conditions, the first three of which are

$$\lim_{Y \to \infty} g'''(Y) = 0, \qquad \lim_{Y \to \infty} g^{\text{iv}}(Y) = 0, \qquad \lim_{Y \to \infty} g^{\text{v}}(Y) = 0. \tag{11}$$

Given the solution $f(Y)$, the function $g(Y)$ can be found by numerically solving the boundary-value problem (9)–(11). The one-parameter family of solutions of this problem we denote as the Stuart-α solutions for turbulent oblique stagnation flow. Note that equation (9) for $g(Y)$ is *linear*. For each solution $f(Y)$ of the Heimenz-α equations there is an associated solution $g(Y)$, and the pair $f(Y), g(Y)$ defines a family of profiles with varying incident angles (8). Since there are at least two solutions for $f(Y)$, there will be at least two solutions of the Stuart-α equations. One solution is regular, converging to Stuart flow as $\alpha \to 0$. Another one is singular, not having a regular limit as $\alpha \to 0$.

2.3. Radially-Symmetric Stagnation-Point Flow

For the sake of completeness, we also analyze radially-symmetric stagnation-point flow. This problem has the greatest practical interest of all stagnation-point flows. Its analysis is completely analogous to the Heimenz-α flow, and hence it may be explained briefly.

Following Homann,[16] we look for the Stokes streamfunction $\Psi(r, z)$ in (r, z) cylindrical coordinates giving the velocities (u_r, u_z) as $(r^{-1}\partial_z\Psi, -r^{-1}\partial_r\Psi)$. The axisymmetric irrotational stagnation-point flow in this system is given by $\Psi = ar^2z$. Upon rescaling the coordinates as $(r, z) = \sqrt{A/a}\,(R, Z)$, a solution is sought in the form $\Psi(R, Z) = \sqrt{A^3/a}\,R^2 f(Z)$. Again matching to the outer flow and requiring no-slip at the impermeable plate yields boundary conditions (4), with Y replaced by Z. Substitution of $\Psi(R, Z)$ into (1) yields the following fifth-order ODE for $f(Z)$,

$$F''' + 2fF'' - (1+\beta)\,f'F' + \beta(f'^2 - \tilde{\alpha}^2 f''^2) + 1 = 0, \tag{12}$$

where $F = f - \tilde{\alpha}^2 f''$ and $\tilde{\alpha}$ retains its definition given in Section 2.1. This Homann-α problem has an analytic solution,

$$f = Z + \tilde{\alpha}(e^{-Z/\tilde{\alpha}} - 1), \tag{13}$$

whose streamlines again form a boundary layer of thickness $\approx \tilde{\alpha}$ near the wall. There is also a regular solution, converging to the Homann solution as $\alpha \to 0$. The spatial behavior of these solutions is similar to the two-dimensional case illustrated in Fig. 1.

3. VON KÁRMÁN-α SWIRLING FLOWS

Von Kármán flow allows one to analyze the effect of rotation in the vicinity of solid walls. For the LANS-α equations, we follow von Kármán[17] in deriving a reduction of the LANS-α equations that describes the swirling motion of a fluid driven by a disc rotating in its own plane. Here cylindrical coordinates (r, z) are used for a disc coincident with the plane $z = 0$ rotating at constant angular velocity Ω about the z-axis. The *ansatz* for the velocity field consistent with the boundary conditions is

$$u_r = r\Omega f(Z), \qquad u_\phi = r\Omega g(Z), \qquad u_z = \sqrt{\Lambda/\Omega}\, h(Z), \tag{14}$$

where $Z = \sqrt{\Omega/\Lambda}\, z$ is the scaled vertical coordinate. Equations (1) yield the following set of ODEs for $f(Z)$, $g(Z)$, $h(Z)$, in which $F = f - \tilde{\alpha}^2 f''$ and $G = g - \tilde{\alpha}^2 g''$,

$$\begin{aligned} &[(1+\beta)\, fF - (1-\beta)\, gG + F'h - F'']' \\ &\qquad = \beta(Ff' + gG' + gF), \qquad 2fG + G'h = G'', \end{aligned} \tag{15}$$

where $2f + h' = 0$ and $\tilde{\alpha} = \alpha\sqrt{\Omega/\Lambda}$. The boundary conditions for (15) are the no-slip conditions at $Z = 0$ and the matching conditions at $Z = \infty$, *viz.*

$$\begin{gathered} f(0) = 0, \qquad g(0) = 1, \qquad h(0) = 0, \\ \lim_{Z\to\infty} f(Z) = 0, \qquad \lim_{Z\to\infty} g(Z) = 0, \qquad \lim_{Z\to\infty} h(Z) = \text{const.} \end{gathered} \tag{16}$$

The vertical velocity function $h(Z)$ tends to a constant as $Z \to \infty$. This corresponds to uniform vertical suction into the boundary layer on the disk.

Equations (15) form a tenth-order system. Boundary conditions at infinity provide additional requirements for the derivatives of $f(Z)$ and $g(Z)$, such as $f'(\infty) = 0$ and $g'(\infty) = 1$. Generalizations of this problem, including the rotation of fluid at infinity, can be considered through use of an alternative scaling and changing the boundary conditions at $Z = 0$ and $Z = \infty$, see ref. 18.

The solutions are obtained by continuation in α starting at $\alpha = 0$ with the von Kármán solution. An example integration showing $h(Z)$ of the von Kármán-α solution for $\alpha = 0.5$ is demonstrated on Fig. 2. We see that increasing α decreases the suction velocity $h(Z = \infty)$. The solution, which can only be obtained numerically, tends to von Kármán's solution as $\tilde{\alpha} \to 0$, and is *regular*, according to the definition in the previous section.

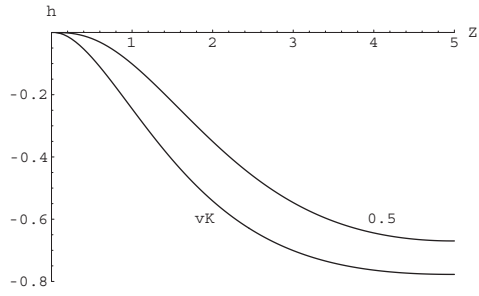

Fig. 2. Velocity function $h(Z)$ for von Kármán-α flow computed for $\tilde{\alpha} = 0.5$. vK: von Kármán's solution ($\alpha = 0$), 0.5: numerical solution for $\alpha = 0.5$.

For the case of von Kármán swirling flows, we have failed to find a singular solution. It is not clear at present whether a singular solution exists for this problem.

4. PRANDTL-α BOUNDARY-LAYER EQUATIONS

4.1. Derivation

In many practical applications, viscous effects of a streamwise flow are confined to a narrow region in the cross-stream direction. The leading order description of these so-called boundary-layer flows may be found by introducing a small parameter which is the ratio of the cross-stream scale to the much larger downstream scale. The resulting boundary-layer equations first introduced by Prandtl,[19] offer a good description of the flow adjacent to solid walls, as well as the flow in narrow jets and wakes. Since this article is concerned with wall effects, it is only natural for us to investigate the LANS-α equations in the limit when boundary-layer flows are present.

Let us assume, for simplicity, that we have a planar (x, y) flow with coordinate velocities (u_x, u_y). Assume the characteristic streamwise velocity is of order U_*, the scale along the streamwise direction x is of order L and the scale in the plate-normal direction y is of order $\delta \ll L$. Upon scaling coordinates according to $x = LX$ and $y = \delta Y$ and streamwise velocity as $u_x = U_* U_x$, the continuity equation gives $u_y = \epsilon U_* U_y$, where $\epsilon = \delta/L$, and the pressure analog q scales as $q = \rho U_*^2 Q$. Balancing viscous diffusion with the leading order convective terms in (1) requires $\delta \sim \sqrt{\Lambda}$. Cheskidov[2] used this re-scaling for (1) to obtain the boundary layer approximation to LANS-α equations. Unfortunately, the boundary-layer equations obtained in ref. 2 do not conserve linear momentum. To correct this perhaps subtle error in Cheskidov's equations, we recall that (1) was derived under the

assumption that $\alpha = \text{const}$. Since α is the Root-Mean-Square (RMS) of the Lagrangian fluctuations, the scale of the fluctuations and therefore α is dependent on the thickness of boundary layer, which varies with the streamwise coordinate x. Thus, one needs to start with the LANS-α equations for variable α. This modifies the Helmholtz operator, but more importantly, it results in the additional term $|\nabla u|^2 \nabla\alpha^2/2$ on the left-hand side of (1); see for example refs. 6, 20, and 21. Re-scaling of this modified LANS-α equation in the thin-layer approximation yields the *Prandtl-α boundary-layer equations*,

$$U_x \frac{\partial V_x}{\partial X} + U_y \frac{\partial V_x}{\partial Y} + \tilde{\alpha}^2 \left(\frac{\partial U_x}{\partial X}\frac{\partial U_x}{\partial Y} - \frac{\partial U_x}{\partial Y^2}\frac{\partial U_x}{\partial X} \right) + \frac{\partial \tilde{\alpha}^2}{\partial X}\left(\frac{\partial U_x}{\partial Y}\right)^2 = -\frac{d\tilde{Q}(X)}{dX} + \frac{\partial^2 V_x}{\partial Y^2}, \tag{17}$$

where $\tilde{\alpha} = \alpha/\delta$ and $V_x = U_x - \tilde{\alpha}^2 \partial^2 U_x/\partial Y^2$, and the pressure analog $Q(X, Y)$ is related to $\tilde{Q}(X)$ by

$$Q(X, Y) + \frac{\beta}{2}\left[U_x^2 - \tilde{\alpha}^2 \left(\frac{\partial U_x}{\partial Y}\right)^2 \right] = \tilde{Q}(X). \tag{18}$$

Observe that the modified pressure $Q(X, Y)$ is not independent of Y, as it is in classical boundary-layer theory, but has an additional dependence on Y due to the term $v_j \nabla u_j$ in (1). This boundary-layer approximation of the NS-α equations defines the Prandtl-α model.

In the version of Prandtl-α equations in ref. 2, obtained by direct application of thin-layer approximation to (1), the pre-factor of the last term of the left-hand side of (17) is equal to $1/2$, and not 1. This has serious consequences for the conservation of momentum, which must be obeyed by any model of turbulent flow. Taking the integral of (17) with respect to y leaves no bulk terms in the absence of external forces. In this case, the change of momentum of any fluid parcel is caused exclusively by the forces acting on the boundaries of this parcel. This is not the case for the version of the Prandtl-α equations in ref. 2, where the bulk term $\frac{1}{2}\int (\partial_y U_x)^2 \partial_x \alpha^2 \, dy$ affects the change of momentum. If $\alpha^2 = \text{const}$, the unphysical generation of momentum due to this term is absent. However, as we show for the examples below, $\alpha(X)$ necessarily grows in proportion to the thickness of boundary layer. Consequently, momentum conservation requires the corrected version of the Prandtl-α equations in (17).

The rest of this section is devoted to two particular applications of the Prandtl-α equations in (17): a turbulent wake and a turbulent jet. These

problems will allow us to connect the predictions of Prandtl-α models with experiments. While the new correction term in Prandtl-α equations drops out of the asymptotic wake problem, for the case of a planar jet the conservation of momentum is crucial.

4.2. Planar Turbulent Wakes

Suppose a slender reflection-symmetric two-dimensional body is immersed in a uniform stream of velocity U_∞ aligned with the x-axis. The body is centered about $y = 0$ and a wake flow develops downstream of the body. Far downstream the velocity deficit $w = U_\infty - u(X, Y)$ will be small, i.e., $w/U_\infty \ll 1$. Here $x = LX$ and $y = \delta Y$ as before. Upon scaling the streamwise and deficit velocities with U_∞, the Prandtl-α boundary layer equations (17) may be linearized to obtain the leading order description,

$$\frac{\partial^2 W}{\partial X\,\partial Y} = \frac{\partial^3 W}{\partial Y^3}, \qquad W = w - \tilde{\alpha}^2 \frac{\partial^2 w}{\partial Y^2}. \tag{19}$$

Following Goldstein[22] we seek a solution in the form $(w(X, Y), W(X, Y)) = X^{-1/2}(f(\eta), F(\eta))$ where $\eta = Y/X^{1/2}$. For similarity, α must grow as the boundary layer thickness, so we set $\alpha(x) = \alpha_0 x^{1/2}$. This self-similar *ansatz* yields the fifth-order system for $f(\eta)$

$$F''' + \tfrac{1}{2}(F + \eta F')' = 0, \qquad f'' - \tilde{\alpha}^2 f = -\tilde{\alpha}^2 F, \tag{20}$$

where $\tilde{\alpha}^2 = \Lambda/(U_\infty \alpha_0^2)$. The boundary conditions are $f(\pm\infty) = 0$ and $f(\eta)$ is even, so $f'(0) = 0$. The solution satisfying these conditions is

$$f(\eta) = C\left[2\cosh(\tilde{\alpha}\eta) - \left\{e^{\tilde{\alpha}\eta}\,\mathrm{erf}\left(\frac{\eta + 2\tilde{\alpha}}{2}\right) - e^{-\tilde{\alpha}\eta}\,\mathrm{erf}\left(\frac{\eta - 2\tilde{\alpha}}{2}\right)\right\}\right]. \tag{21}$$

Here C is adjusted so that $f(0) = 1$ for comparison with experimental results. The agreement of this Prandtl-α solution with experimental data of Townsend[24] and Wygnanski *et al.*[23] is presented in Fig. 3. For comparison, we also display the empirical result $f(\eta) = \exp(-0.693\eta^2)$ traditionally used in describing the velocity profile (see Schlichting,[11] p. 743).

4.3. Planar Turbulent Jets

The Prandtl-α equations for the case of a planar turbulent jet conserve the momentum flux $J_0 = \int_{-\infty}^{+\infty} U_x V_x \,\mathrm{d}y$. The dimensions of J_0 are L^3/T^2. Since the length scale in the planar jet is growing linearly with X,[11] we choose length scale $l_* = X$ and velocity scale at a given position X as

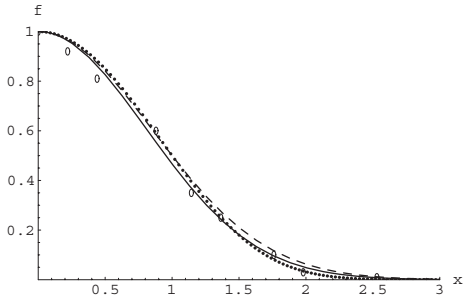

Fig. 3. Comparison of analytical solution (21) (solid line) with experimental data of Wygnanski *et al.*[23] (dots) and Townsend[24] (circles). The dashed line represents the traditional Gaussian fit $f(\eta) = \exp(-0.693\eta^2)$ in Schlichting,[11] p. 743.

$u_* = \sqrt{J_0/X}$. Then the sole choice for the dissipation coefficient is $\Lambda \sim \sqrt{J_0 X}$. Here conservation of momentum was crucial for choosing the scales, so consideration of the free jet flow could not be accomplished using the Prandtl-α model equations in ref. 2 derived using a constant value of α.

We posit a self-similar solution for the streamfunction in the form $\psi(X, Y) = \sqrt{J_0 X}\, f(y/X)$ with $\alpha(X) \sim X$, and choose the width of the turbulent jet to satisfy $\delta(X) \sim X$, consistent with experiments.[11] The similarity function $f(\eta)$ is odd $f(\eta) = -f(-\eta)$ and satisfies the fifth-order ordinary differential equation

$$f''^2 + 2ff''' + ff^{\mathrm{iv}} - f'^2 - ff'' = f''' - f^{\mathrm{v}}. \tag{22}$$

Boundary conditions for $f(\eta)$ are $f(\eta) \to f_0$ when $\eta \to \infty$. The constant f_0 is found as part of the solution. All the coefficients were removed from (22) by re-scaling η. Integrating (22) twice and using the aforementioned boundary conditions, we obtain

$$ff'' - \tfrac{1}{2} f^2 = f' - f''' - \tfrac{1}{2} f_0^2. \tag{23}$$

All the experimental results in the literature are presented with the velocity at $\eta = 0$ being normalized to unity; therefore, we require $f'(0) = 1$. From the condition $f(\eta) \to f_0$ when $\eta \to \infty$ we find numerically $f_0 \simeq 1.806$. There is no remaining parametric freedom in the solution of (23). Figure 4 shows its agreement with the experimental data of Gutmark and Wygnanski.[25]

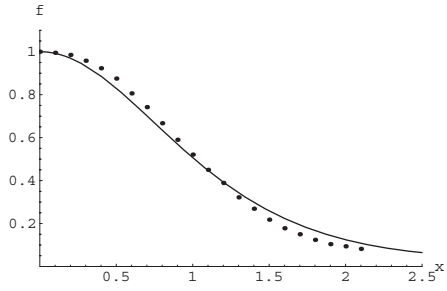

Fig. 4. Comparison of the numerical solution of (23) (solid line) with data of Gutmark and Wygnanski[25] (dots).

5. SUMMARY

In this short paper, we have reported the following observations.

- Boundary conditions for the LANS-α equations in a bounded domain do not necessarily apply in a semi-infinite domain for solutions with infinite energy. Our analytical solutions provide guidelines for choosing these properly.
- In semi-infinite domains, multiple solutions with infinite energy exist for LANS-α. Examples of this were already known for the Navier–Stokes equations.
- We introduced the Prandtl-α approximation so as to preserve conservation of linear momentum and we discussed exact solutions of the Prandtl-α equations for turbulent jets and wakes.

ACKNOWLEDGMENTS

We are grateful to A. Cheskidov and E. S. Titi for discussions. We are also grateful for helpful suggestions from the referees. D.D.H. and B.W. were supported by DOE, under contract W-7405-ENG-36. V.P. was partially supported by Sandia National Laboratory SURP grant.

REFERENCES

1. J. E. Marsden and S. Shkoller, *Proc. Roy. Soc. London* **359**:1449–1468 (2001).
2. A. Cheskidov, *C. R. Acad. Sci. Paris, Ser. I* **334**:423–427 (2002).
3. S. Chen, C. Foias, D. D. Holm, E. Olson, E. S. Titi, and S. Wynne, *Phys. Rev. Lett.* **81**:5338 (1998); *Phys. Fluids* **11**:2343 (1999); *Physica D* **133**:49 (1999).
4. T. Wei and W. W. Willmarth, *J. Fluid Mech.* **65**:439 (1974).
5. M. V. Zaragola, Ph.D. thesis (Princeton University, 1996).

6. V. Putkaradze and P. D. Weidman, Turbulent wake solutions of the Prandtl-α equations, *Phys. Rev. E* **67**:036304 (2003).
7. J. Leray, *Acta Math.* **63**:193 (1934).
8. D. D. Holm, J. E. Marsden, and T. S. Ratiu, *Phys. Rev. Lett.* **349**:4173–4177 (1998).
9. D. D. Holm, J. E. Marsden, and T. S. Ratiu, *Adv. in Math.* **137**:1–81 (1998).
10. C. Foias, D. D. Holm, and E. S. Titi, *Physica D* **152–153**:505 (2001); Ibid, *Dynam. and Differential Equations,* **14**:1 (2002).
11. H. Schlichting, *Boundary Layer Theory*, 7th ed. (McGraw–Hill, 2000).
12. K. Heimenz, *Dingl. Polytech. J.* **326**:321 (1911).
13. J. T. Stuart, *J. Aero/Space Sci.* **26**:124 (1959).
14. K. Tamada, *J. Phys. Soc. Japan* **46**:310 (1979).
15. J. M. Dorrepaal, *J. Fluid Mech.* **163**:141 (1986).
16. F. Homann, *ZAMM* **16**:153 (1936).
17. T. von Kármán, *ZAMM* **1**:233 (1921).
18. U. T. Bödewadt, *ZAMM* **20**:241 (1940).
19. L. Prandtl, in *Ayerodynamic Theory III*, W. F. Durand, ed. (1936), p.16.
20. D. D. Holm, *Physica D* **133**:215 (1999).
21. J. E. Marsden and S. Shkoller, *Arch. Rational Mech. Anal.* **166**:27–46 (2003).
22. S. Goldstein, *Modern Developments in Fluid Dynamics* (Dover, 1965).
23. I. Wygnanski, F. Champagne, and B. Marasli, *J. Fluid Mech.* **168**:31 (1988).
24. A. Townsend, *Proc. Roy. Soc A* **197**:124 (1949).
25. E. Gutmark and I. Wygnanski, *J. Fluid Mech.* **73**:465 (1976).